On the transport, variability and origin of dense water masses crossing the South Scotia Ridge

Michael P. Schodlok, Hartmut H. Hellmer, Aike Beckmann

Alfred Wegener Institute for Polar- and Marine Research, Bremerhaven, Germany

Abstract

The deep Scotia Sea is filled with ventilated Weddell Sea Deep Water. This in turn is an essential contributor to the ventilation of the World Ocean abyss. Depending on the formation process and/or its location along the Weddell Sea periphery, deep and bottom water masses follow different routes to cross the South Scotia Ridge. A primitive equation, hydrostatic, terrain-following coordinate ocean general circulation model (BRIOS-1) is used to investigate the water mass export from the Weddell Sea. The model is circumpolar focusing on the Weddell Sea, with particularly high resolution ($\sim$ 20 km) in the DOVETAIL area. 24 x 10^6 m^3s^{-1} of eastward Weddell Sea Deep Water transport is found in the northern limb of the Weddell Gyre across 44°W. Export rates of Weddell Sea Deep Water through gaps in the South Scotia Ridge are estimated to be 6.4 x 10^6 m^3s^{-1} with a semi-annual cycle of $\pm$ 0.6 x 10^6 m^3s^{-1} which can be correlated to atmospheric cyclone activity and Weddell Gyre strength. Sensitivity studies considering extreme sea ice conditions in the Weddell Sea show higher (lower) exports in years of minimum (maximum) winter sea ice extent. Lagrangian particle trajectories illustrate the pathways of water masses from the inner Weddell Sea into the Scotia Sea through various gaps in the South Scotia Ridge. They highlight the existing flow divergence on the northwestern continental shelf with one branch entering Bransfield Strait and the other continuing eastwards subsequently filling the deep Weddell and Scotia seas. Water masses flowing through the major gaps originate from the southwestern and southeastern Weddell Sea continental shelves. However, water masses formed east of the Weddell Sea (e.g., Prydz Bay) also seem to feed the deep Scotia Sea, since a large portion of floats flowing northward through the gaps of the South Scotia Ridge have been in contact with the mixed layer processes outside the inner Weddell Sea.

Key words:

Email address: `mschodlok@awi-bremerhaven.de` (Michael P. Schodlok,

1 Introduction

The topographic map of the Atlantic sector of the Southern Ocean reveals an arc shaped ridge system connecting South America and Antarctica (Fig. 2). It totally encloses the Scotia Sea except to the west where Drake Passage allows for deep water inflow from the Pacific sector via the Antarctic Circumpolar Current (ACC). Thus, the Scotia Sea is bounded to the south by the South Scotia Ridge (SSR), to the north by the North Scotia Ridge (NSR), and to the east by the South Sandwich Island Arc. Immediately to the east of the latter, the South Sandwich Trench with the greatest depth ($\sim$ 8200 m) measured in the South Atlantic Ocean serves as the only escape route for bottom water newly formed in the Weddell Sea (Georgi, 1981). The topography of the very rugged ridge system plays an important role in the flow of the ACC from the Pacific to the Atlantic through Drake Passage and in the spreading of deep and bottom waters from the Weddell Sea into the World Ocean.

The Weddell Sea is traditionally regarded as one of the main locations for deep and bottom water formation around Antarctica due to enhanced atmosphere–ice–ocean interaction (Brennecke, 1921; Gill, 1973; Carmack, 1977). Weddell Sea Deep Water (WSDW), a mixture of Warm Deep Water (WDW) and the newly formed Weddell Sea Bottom Water (WSBW), which is called Antarctic Bottom Water (AABW) outside the Weddell Sea spreads from the Weddell Sea into the World Ocean to contribute to the ventilation of its abyss. In the Weddell Sea, ventilated waters flow northward with the deep western boundary current as part of the Weddell Gyre hugging the continental slope east of the Antarctic Peninsula. The SSR effectively hampers an advance farther north and deflects most of the bottom flow to the east. Therefore, one question addressed in this paper is how much WSDW escapes into the Scotia Sea through the deep passages of this ridge system (Fig. 2).

As part of the DOVETAIL experiment, which was designed to determine deep and bottom water pathways, water mass characteristics, and spatial and temporal variabilities (for details see Muench and Hellmer (2001)), this modelling effort concentrates on answering the questions of transport rates, variabilities, and origin of waters flowing through gaps within the SSR. Our ocean model, as part of a modelling effort of the Southern Ocean, will also be used to investigate pathways previously unnoticed or unsampled, and by means of Lagrangian trajectories to identify the origin of waters found in the bottom layers of the Scotia Sea.

This paper describes the design of the model in section 2. The model results are presented in three ways:
(1) hydrographic characteristics for the SSR region are shown and compared to

Hartmut H. Hellmer, Aike Beckmann).

recent observations (e.g., Schröder et al. (2001)) to validate the model output (section 3);

(2) transport rates through various passages in the SSR and their sensitivity to varying forcing fields are investigated (section 4);

(3) modelled float trajectories are used to reveal pathways across the SSR and the origin of water masses found in the deep Scotia Sea (section 5).

A discussion and summary is presented in section 6.

2 Model description

The ocean circulation model (BRIOS-1) belongs to a family of hydrostatic, primitive equation ocean circulation models in the framework of BRIOS (Bremerhaven Regional Ice Ocean Simulations) (Beckmann et al., 1999). BRIOS-1 is a modified version of SPEM (Haidvogel et al., 1991), employs a generalized, nonlinear, terrain-following coordinate system and provides, with 24 vertical layers, enhanced resolution near the sea surface and the sea floor. Thus, this setup seems ideal for studies of shelf dynamics and bottom boundary layer flows.

The model solves the hydrostatic, primitive equations with a rigid lid approximation at the sea surface. It uses advection/diffusion equations for potential temperature and salinity, and the nonlinear UNESCO equation of state, modified by Jackett and McDougall (1995) to accurately represent the density structure at low temperatures on the Antarctic continental shelves including the sub-ice shelf cavities. Ice shelf-ocean interaction in these cavities is included following the description by Hellmer et al. (1998).

The configuration of the model consists of a circumpolar domain extending from 50°S to 82°S including major ice shelves like Filchner-Ronne and Ross as well as the shallow continental shelves of the Weddell and Ross seas (Figure 1). The major ice shelves are represented with as much topographic detail as possible (Johnson and Smith, 1997) whereas the other ice shelves (Larsen, Brunt, Riiser-Larsen, Fimbul and Amery) are included in a coarse resolution due to lack of data. As part of the DOVETAIL experiment, this model focuses on the Weddell Sea sector of the Southern Ocean and in particular on its northern boundary. This is achieved with a high horizontal resolution (20°W to 60°W) in the vicinity of the SSR of 20 km by 20 km. The meridional resolution (0.18°) reduces gradually towards the north and south while the zonal grid spacing of 0.3° within the high resolution area decreases rapidly (within 10 grid boxes) to 5.75°. With this horizontal resolution the model is not eddy resolving as the Rossby radius of deformation in this region is between 5 and 10 km.
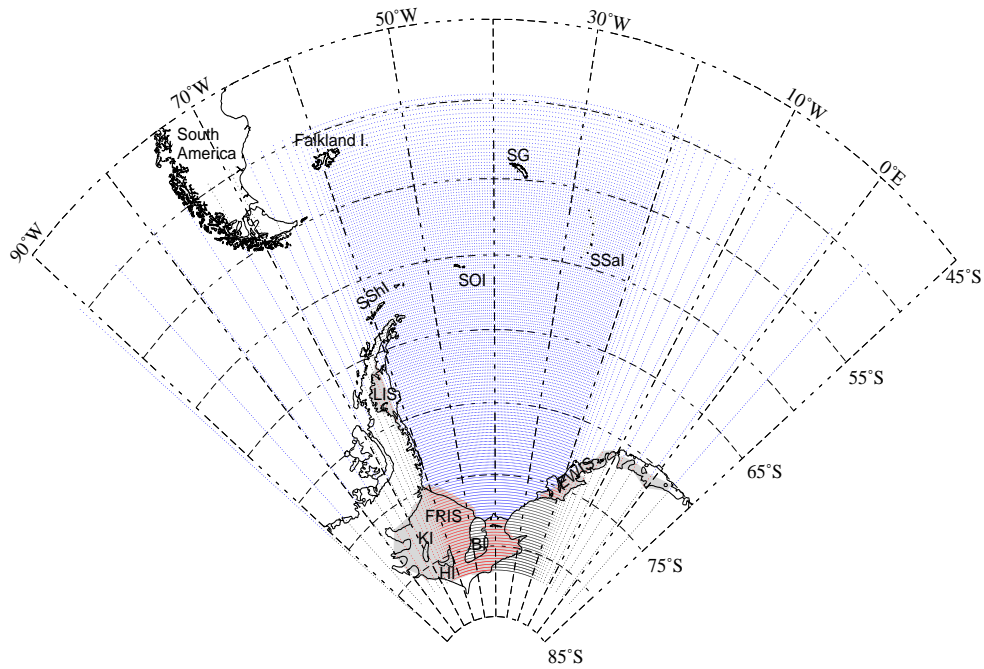
Fig. 1. Sub-domain of the circumpolar model grid BRIOS1.1 focused on the DOVE-TAIL area at a high resolution of 20 km x 20 km. The area of ocean grid points beneath the ice shelves is shaded. FRIS - Filchner–Ronne Ice Shelf with islands BI - Berkner Island, HI - Henry Ice Rise, and KI - Korff Ice Rise, LIS - Larsen Ice Shelf, and EWIS - Eastern Weddell Ice Shelves comprising Riiser-Larsen, Brunt and Fimbul Ice shelves.

The bathymetry data were derived from the Smith and Sandwell (1997) 2' gridded data set north of 72°S, and BAS/AWI data south of that latitude. The minimum water column thickness was set to 200 m, and the r–value (Beckmann and Haidvogel, 1993) limited to 0.2 except for the ice shelf edge, where maximum values of 0.3 were permitted. As Figure 2 shows, the most important features such as the South Scotia Ridge, Powell Basin, and all major passages are well resolved in extent and depth. They match, although interpolated and smoothed onto the grid the measured depth fairly closely (Naveira Garabato, pers. comm.).

Eight islands are included within this area of high resolution; three are sub-ice shelf islands beneath the Filchner–Ronne Ice Shelf (Berkner Island, Korff and Henry Ice Rises), the remaining five islands in the Atlantic sector of the Southern Ocean are the Malvinas, South Georgia and South Orkney islands, and the South Shetland and South Sandwich Island complexes.

At the northern boundary of the model domain the Antarctic Circumpolar Current transport had to be prescribed due to the northward limitation of the model domain. The ACC transport through Drake Passage is set to 130 Sv (1 Sv = 10^6 m³ s⁻¹), in accordance with the observations of Whitworth and
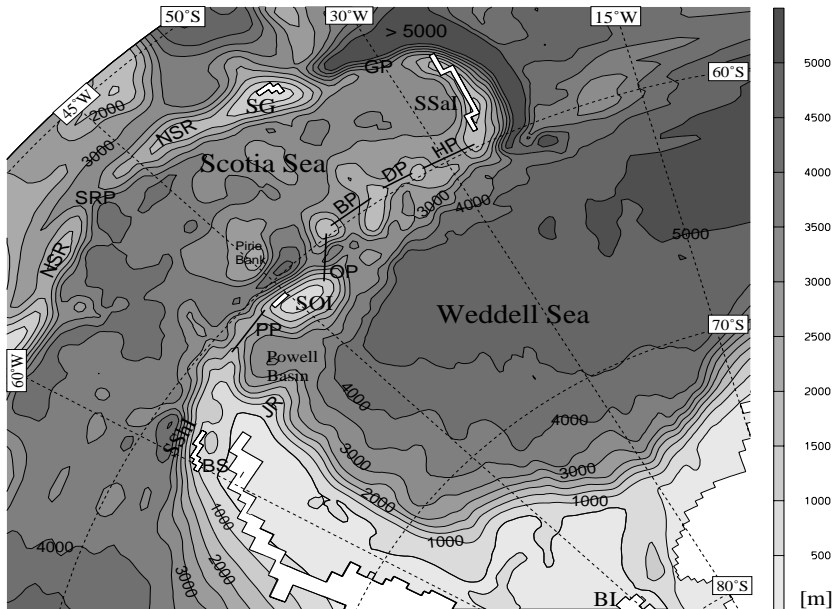
4

Fig. 2. Model bathymetry (isobaths in 500 m intervals) for the Scotia Sea and the inner Weddell Sea. Topographic gaps in the South Scotia Ridge are indicated by their initials: PP – Philip Passage, OP – Orkney Passage, BP – Bruce Passage, DP – Discovery Passage, HP – Hoyer Passage. The islands indicated by their initials are: SG – South Georgia, SSaI – South Sandwich Islands, SOI – South Orkney Islands, SShI – South Shetland Islands. Features of the North Scotia Ridge (NSR) are: GP – Georgia Passage, SRP – Shag Rock Passage. BS – Bransfield Strait, JR – Joinville Ridge.

Peterson (1985). Sixty-five Sv leave the domain between South America and 26°W and are gradually fed back into the Indian Ocean sector between 102°E and 180°E.

Subgrid-scale parameterizations

The functional form of subgrid-scale schemes have been adopted from Beckmann et al. (1999).

Harmonic viscosity and diffusivity operators are used with spatially varying coefficients. The lateral viscosity was chosen to be a linear function of the horizontal grid spacing Δ,

$$\nu_{u,v} = 0.1 \text{ m s}^{-1} \, \Delta$$

A linear boundary layer stress is also applied to the seafloor and the base of the ice shelves.

The lateral diffusivity depends linearly on the local Reynolds number. At the surface and the bottom an additional grid-spacing-dependent background

diffusivity of

$$\nu_{T,S} = 0.01 \text{ m s}^{-1} \ \Delta$$

was added to represent the wind-induced, near surface mixing and enhanced levels of turbulence in the bottom boundary layer.

Vertical viscosity and diffusivity are computed as Richardson-number-dependent functions, according to Pacanowski and Philander (1986). This includes a maximum diffusivity of $\kappa = 0.01 \text{ m}^2 \text{ s}^{-1}$ in case of small and negative Richardson numbers (static instability) . An explicit scheme has been employed for the vertical diffusivity.

Time stepping

The model time step is mainly limited by vertical advection over the shallow continental shelf areas; it is set to 3.6 min (400 time steps per day). For simplicity, the year consists of 12 months with 30 days each.

For the first time, a multigrid elliptical solver (de Zeeuw, 1990) for the stream-function is implemented in an ocean model. This solver has a convergence rate which is not impaired by varying coefficients and complex model geometry as is the case in this model (Rakowsky, 1999) and thus allows a high scalability on parallel computers.

Experimental settings

The ocean circulation model is initialised with data from the Hydrographic Atlas of the Southern Ocean (HASO) (Olbers et al., 1992). Strong restoring of temperature and salinities to the HASO climatology occurs in a buffer zone of 8 grid points at the northern boundary and outside the high resolution area of the model domain. A 'stand-alone' sea-ice/mixed layer model (BRIOS-0) based on Hibler (1979) and Lemke et al. (1990) provided the surface forcing data for the ocean model; the ice model was run on the same horizontal grid as the ocean model forced with the ECMWF reanalysis data from the period 1985 to 1993. The results were monthly averaged to a 'climatological' year which includes the seasonal cycle of sea surface temperature (SST), freshwater flux, and surface stress, all mainly controlled by the seasonality of the modelled sea ice distribution.

The reference run (referred to as RR) with the 'climatological' forcing is integrated for 30 years, although the model reaches a quasi steady state after 15 years. The remaining interannual trends in domain-average temperature and

salinity are small, $3 \cdot 10^{-5}$ °C a^{-1} and $2 \cdot 10^{-5}$ a^{-1}, respectively. In addition to the RR, two sensitivity experiments were performed each using the monthly forcing of a year with extreme sea ice conditions. Starting from RR year 20 they were integrated for an additional 10 years to obtain a quasi steady state. The two years were chosen based on the sea ice model SST data which showed minimum/maximum winter sea ice extent in winter 1990/1992 (referred to as Y90/Y92), indicating the influence of the Antarctic Circumpolar Wave (ACW) (White and Peterson, 1996; Comiso and Gordon, 1998).
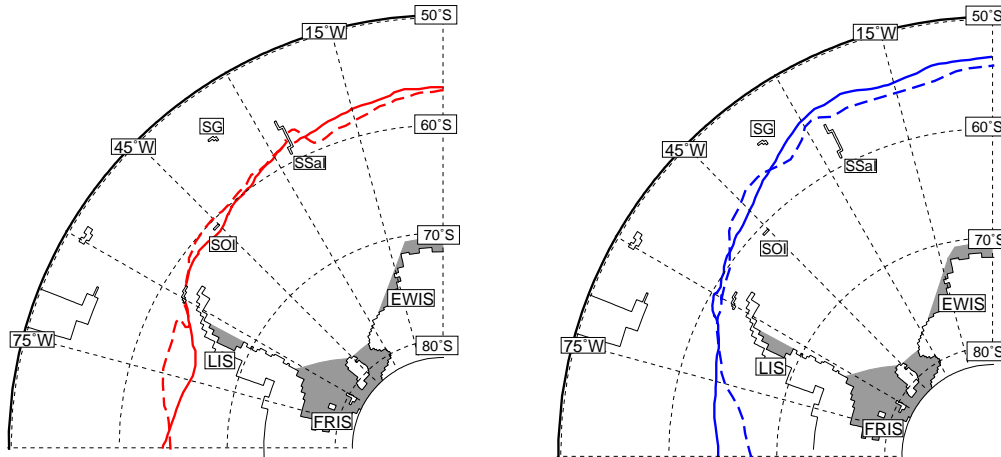

Fig. 3. Monthly mean sea ice extent for 1990 (left) and 1992 (right) indicating the maximum sea ice extent in September of each year. The solid line represents the modelled -1.86°C isotherme representative for the transition from sea ice growth to melting; the dashed line represents the 15 % sea ice concentration of SSM/I PELICON data [Heygster et al., 1996] and thus the sea ice edge. Ice Shelves are shaded with abbreviations as in Fig. 1.

Figure 3 shows the sea ice extent in winter of Y90 and Y92 in the high resolution model area. This Figure depicts the sea ice extent based on SSM/I observations and the modeled -1.86°C isotherm indicating surface freezing temperature and thus the sea ice boundary. Surface forcing data and observations agree well during the time of maximum ice extent. Within the Atlantic sector of the Southern Ocean the northernmost sea ice extent is found. Easterly winds transport sea ice into the Weddell Sea resulting in an accumulatation of sea ice, which is transported to the north by the Weddell Gyre causing thus the maximum sea ice extent in the northwestern Weddell Sea/Scotia Sea. In 1990, however, northeasterly winds blocked this northward sea ice transport establishing the sea ice edge near 56°S. In 1992, southwesterly winds supported sea ice transport farther north into the Scotia Sea to about 60°S.

A 3-day data set of temperature, salinity, velocity components, and transport streamfunction obtained from the 31st year of integration was used for further model analysis and 'offline' experiments, e.g., to calculate Lagrangian trajectories of particles released in the model water column.

3 Model results

This section presents the main characteristics of the modeled hydrography and circulation. An assessment of the results is performed by quantitative comparison with observations.

Figure 4 shows the annual mean bottom potential temperature distribution of the Weddell and Scotia seas after 30 years of integration which match well with the climatology of bottom potential temperatures shown by Locarnini et al. (1993). Water cooler than 0.2°C does not enter the Scotia Sea from the west (Drake Passage) and thus Scotia Sea waters below 0.0°C, i.e., water with WSDW characteristics, derive solely from the Weddell Sea through gaps in the SSR. Figure 4 also shows that WSDW escaping the Weddell Sea via the South Sandwich Trench does enter the Scotia Sea from the east via Georgia Passage (GP in Figure 2) indicated by a tongue of cold water leaking into the Scotia Sea. Bottom potential temperatures in the southeastern Scotia Sea are slightly too warm indicating that even a horizontal resolution of 20 km across the South Scotia Ridge does not resolve all possible passages of the ridge system. In fact, Naveira Garabato et al. (2001a) show narrow gaps in the eastern part which might allow cold water to spread into the Scotia Sea contributing to the cold bottom water found in the climatology of Locarnini et al. (1993).
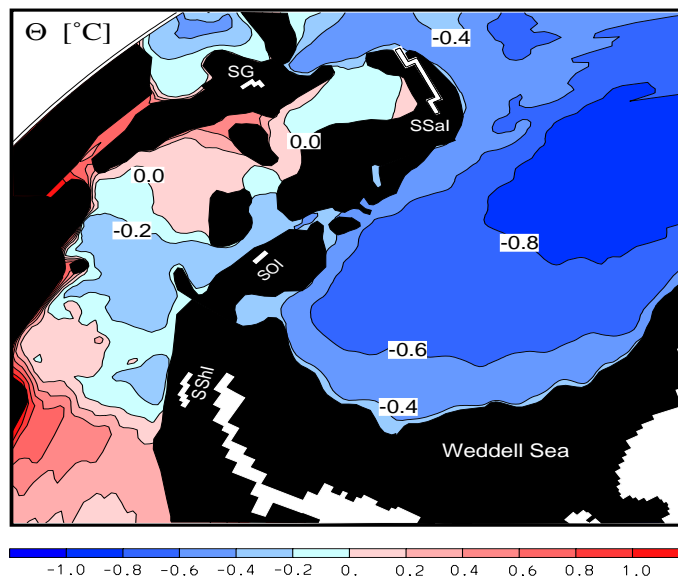

Fig. 4. Modelled bottom potential temperature of the high resolution area for depths greater 3000 m.

A zonal section of modelled temperature and salinity along the western SSR (Figure 5) exhibits at mid-depth the Warm Deep Water represented by its warm ($\Theta > 0.3$°C) and salty (S > 34.685) cores. Lower Circumpolar Deep Water (LCDW) is fed into the Weddell Gyre at around 20°E and transformed
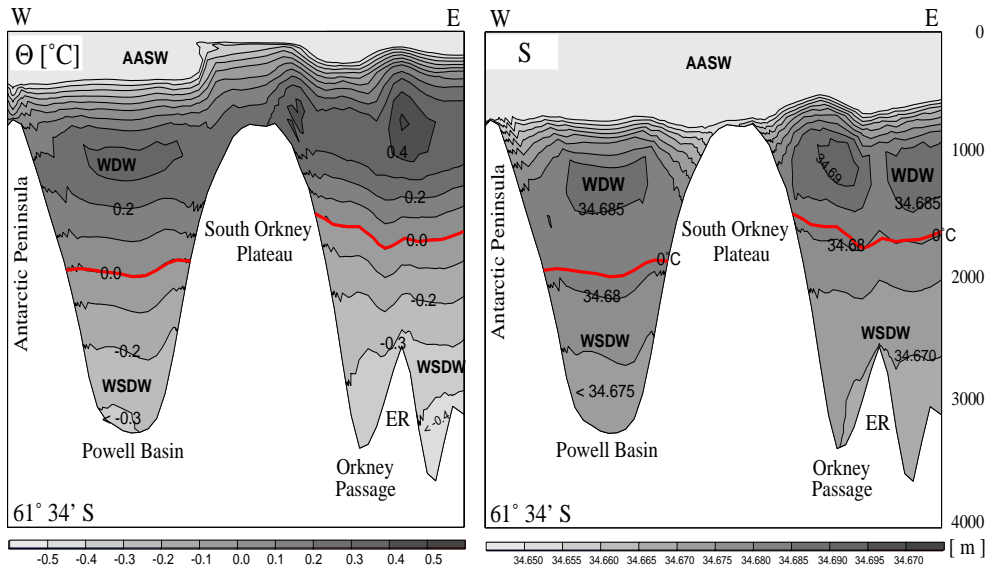
Fig. 5. Zonal potential temperature (left) and salinity (right) section across the South Scotia Ridge at 61°34' S. Labeled are the main water masses, Antarctic Surface Water (AASW), Warm Deep Water (WDW), and Weddell Deep Water (WSDW). ER indicates the northward extension of the Endurance Ridge. The dark line (0°C isotherm) indicates the mean upper bound of WSDW in both sections.

due to mixing to WDW (Schröder and Fahrbach, 1999). In the Weddell Sea, the maxima for Θ and S occur at 300 m and 500 m depth, respectively, except close to the continental shelf where the WDW core is found deeper in the water column (down to 1000 m) due to onshore Ekman flow (Whitworth et al., 1998).

Weddell Sea Deep Water is found below the WDW throughout the Powell Basin, occupying a depth interval between 2000 m and 4000 m. A core of colder water is hugging the western slope of the basin possibly being a diluted remnant of newly formed Weddell Sea Bottom Water. Although WSBW occupies the bottom layer throughout the western Weddell Sea the coldest water mass in Orkney Passage ($\Theta < -0.4°C$) is associated with WSDW as found recently by Schröder et al. (2001) (see Table 1 for Weddell Sea water mass characteristics).

The horizontal velocity distribution at 500 m depth (Figure 6) depicts the ACC and its fronts entering the Scotia Sea through Drake Passage as well as the northern branch of the Weddell Gyre associated with the Weddell Front. The Subantarctic Front (SAF) as the northern most front of the ACC turns into the South Atlantic establishing the Malvinas Current. The southern Boundary (SB) of the ACC, called Scotia Front within the Scotia Sea, enters the South Atlantic just northwest of the South Sandwich Islands and immediately turns south east of the islands. ACC velocities associated with the fronts and locations of the fronts agree well with observed values and positions (Orsi et al., 1995).

Table 1
Water Mass characteristics of the Weddell Sea.

Water mass	Acronym	Θ [°C]	S
Antarctic Surface Water	AASW	-1.7 − 2.0	< 34.3
Winter Wasser	WW	< -1.7	34.3 − 34.45
Circumpolar Deepwater	CDW	0.2 − 0.8	34.66 − 34.8
Warm Deepwater	WDW	0.0 − 0.8	34.6 − 34.72
Weddell Sea Deep Water	WSDW	-0.7 − 0.0	34.64 − 34.7
Weddell Sea Bottom Water	WSBW	< -0.7	34.62 − 34.66

Sources: Carmack und Foster, (1975); Reid et al., (1977); Foldvik et al.,
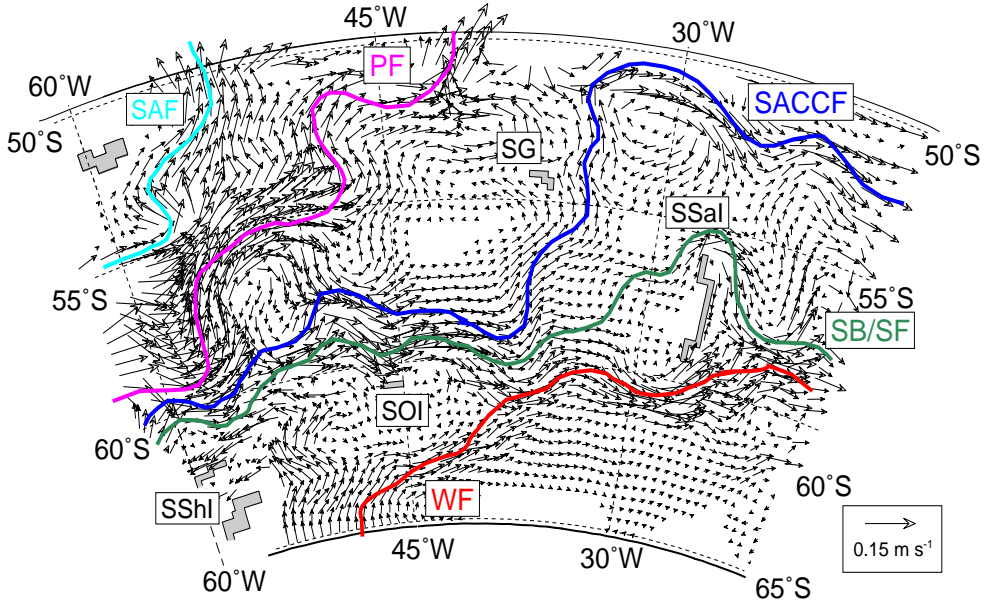(1985); Grosfeld et al., (2001).

Fig. 6. Horizontal velocity field of the Scotia Sea at 500 m depth. Velocity vectors
represent flow between 0.05 m s^{-1} and 0.15 m s^{-1}. The ACC fronts are Subantarc-
tic Front (SAF), Polar Front (PF), Southern ACC Front (SACCF), and Southern
Boundary/Scotia Front SB/SF. In the northern Weddell Sea the Weddell Front
(WF) as northern boundary of the Weddell Gyre is plotted.

The horizontal velocity distribution at 2750 m depth (Figure 7) represents
the main features of the Weddell Sea circulation. As part of the southern
limb of the Weddell Gyre, the coastal current adheres to the slope of the
Antarctic continental shelf entering the inner Weddell Sea from the east. On
its way around the inner Weddell Sea, the strength of the coastal current
diminishes but increases again as it approaches the northern extension of the
Antarctic Peninsula. Here, two branches evolve, the coastal current progressing
westwards north of the South Shetland Island complex and a strong boundary
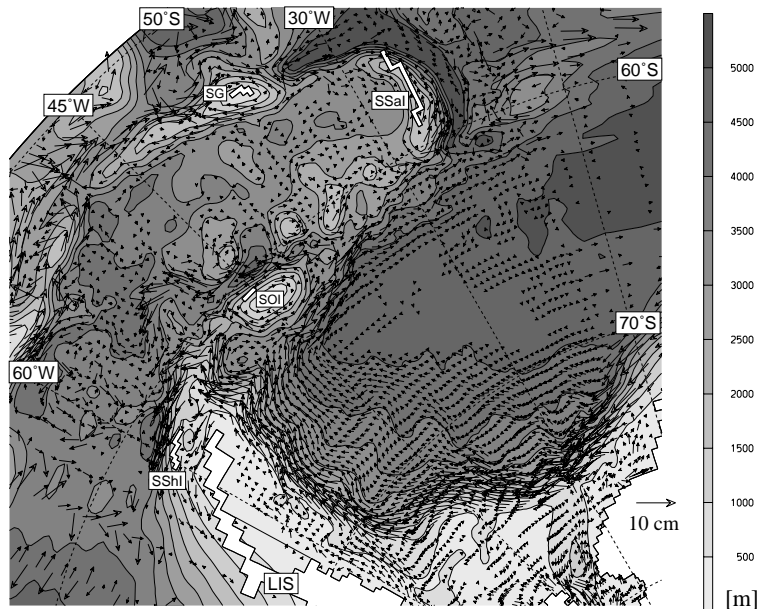
10

Fig. 7. Horizontal velocity field at 2750 m depth and model bottom topography contour interval 500 m. Velocity vectors represent flow between 0.02 m s^{-1} and 0.1 m s^{-1}.

current at the southern slope of the SSR. The latter has been observed by lowered Acoustic Doppler Current Profiler (LADCP) measurements southeast of the South Orkney Plateau (Gordon et al., 2001). We compute the model mean WSDW transport within the northern limb of the Weddell Gyre to be 24 Sv which agrees with the LADCP based value of 25 Sv. WSBW associated with this deep current cannot cross the ridge and thus is forced to flow along the base of the SSR into the deep Weddell Basin (Orsi et al., 1993).

The upper layers are dominated by eastward flow associated with the ACC. However, observations (Gordon, unpublished cruise report) and our model results (Figure 7) show a strong westward flow in the bottom layers at the northern slope of the South Scotia Ridge.

To the north, the fast flowing and deep reaching Antarctic Circumpolar Current bends southwards east of the South Sandwich Islands, thus obstructing the northward advance of WSDW and WSBW in the South Sandwich Trench (Locarnini et al., 1993). The velocity field shows a circulation which splits in Georgia Passage between South Georgia (SG) and South Sandwich Islands (SSaI). Close to SG water flows into the Georgia Basin towards the north/northeast and subsequently into the Argentine Basin (Smythe-Wright and Boswell, 1998). As inferred from the bottom potential temperatures, the velocity field indicates a south/southeast flow west of SSaI into the Scotia Sea being responsible for the eastern tongue of cold water.

11

4 Transports and transport variability

This section presents the overflow transports of WSDW through deep passages in the South Scotia Ridge into the Scotia Sea.

Philip Passage

Philip Passage ($\sim$ 47°W, Fig. 2), located between Clarence and Signy islands south of Hesperides Trough, is the deepest gap in the South Scotia Ridge west of the South Orkney Plateau. The model depth of 2050 m is slightly deeper than the observed depth ($\sim$ 1980 m), but seems to be appropriate to study deep water overflow.

Although being shallower than, e.g., Orkney Passage, Philip Passage overflow water is identified as WSDW. Over a one year period, the reference run (RR) export rates (Figure 8a) into the Scotia Sea show a seasonal cycle with maxima in April and October at a rate of 2.4 Sv each (annual mean 2.2 Sv). The sensitivity runs indicate the same seasonal cycle with little interannual transport differences. Y92 shows a slight decrease in annual mean transport (2.0 Sv) but an increase in seasonal variation (40 %), and, compared with RR, a shift of the maxima towards earlier dates by 2 weeks and 2 months, respectively. Y90 shows a small increase in mean transports (2.3 Sv) but the largest maxima (2.6 Sv).

Philip Passage transports and WSDW transport in the Weddell Gyre are weaker correlated for Y92 (0.61) than for Y90 (0.83). This smaller correlation indicates that transports of water masses leaving the northwestern continental shelf reduce the influence of Weddell Gyre waters entering Powell Basin. In addition, during years of minimum winter sea ice extent (Y90) shelf dynamics seem less influential on SSR overflow.

Orkney Passage

The Orkney Passage (40°W) east of the South Orkney Plateau is the deepest gap in the South Scotia Ridge with a sill depth of around 2900 m allowing throughflow of deep and possibly bottom waters (Gordon, 1966; Locarnini et al., 1993). Although this is long known, transport rates of WSDW into the Scotia Sea still have to be determined.

The model reference run yields a mean northward transport of 4.2 Sv through Orkney Passage with seasonal maxima in April and August, the latter being
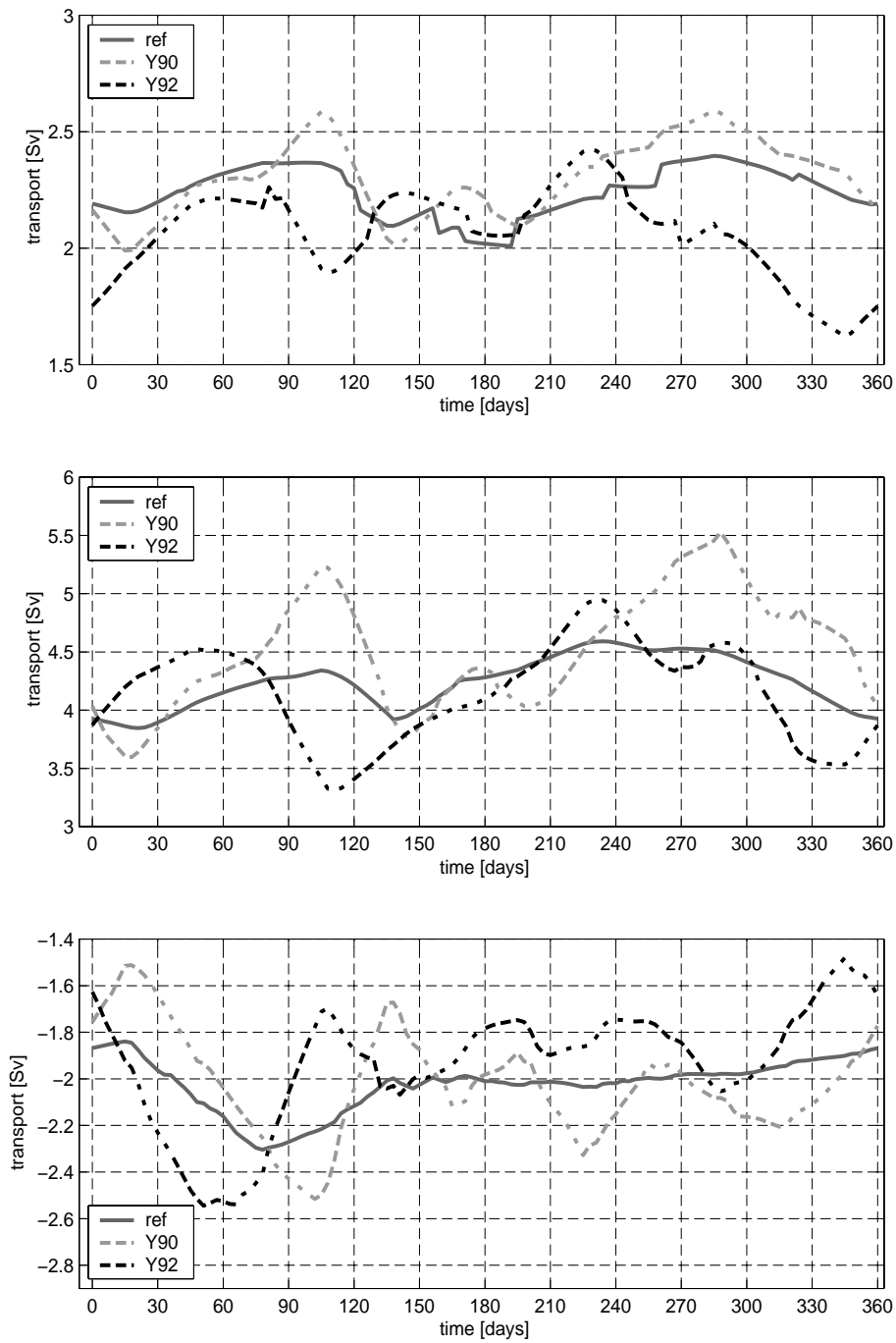
Fig. 8. Integrated transports through Philip Passage (a), Orkney Passage (b), and Bransfield Strait (c). Reference run (RR): solid line, sensitivity run Y90 (atmospheric forcing with minimum winter sea ice extent): short dashed, sensitivity run Y92 (atmospheric forcing with maximum winter sea ice extent): long dashed, Positive values in (a) and (b) indicate northward transport, negative values in (c) indicate westward transport.

0.3 Sv larger (Fig. 8b). This correlates extremely well with the variability of ECWMF 10-m wind velocities (G. Birnbaum, pers. comm.) and with WSDW

transports of the Weddell Gyre (normalized cross correlation of 0.94 without phase shift).

Thus, the Orkney Passage transport is determined by the WSDW transport in the Weddell Gyre which, in turn, is strongly influenced by the winds. In addition, observations by Fahrbach et al. (1992) showed similar seasonalities within the coastal current off Kapp Norvegia. Our transport rates seem to be reasonable as model bottom velocities of 0.04 m s^{-1} within Orkney Passage agree with LADCP derived velocities (Gordon, unpublished cruise report, 1997). Although northward flow into the Scotia Sea dominates, a reverse flow into the Weddell Sea at the eastern flank of the passage also occurs in agreement with the observations of Naveira Garabato et al. (2001b).

The sensitivity studies, as described in section 2, reveal an interannual variability of passage throughflow. The Y90 model results show higher annual–mean transports through Orkney Passage than the Y92 results; 4.5 Sv vs. 4.1 Sv. In addition to these transport differences, a shift in the peak of throughflow also exists. While in Y90 the Orkney Passage transport maxima occurred in April and October (5.2 Sv and 5.5 Sv, respectively), the maxima in Y92 occured about 2 months earlier in February and August (4.5 Sv and 4.9 Sv, respectively). However, the normalized cross correlation between the Weddell Gyre and Orkney Passage transports, with values of 0.87 (Y90) and 0.85 (Y92), reveal a phase shift of only one (Y92) and two weeks (Y90). This confirms that the WSDW transport within the Weddell Gyre has a very large influence on the passage transports.

Transports through Philip Passage and Orkney Passage both show a semi-annual cycle, although of different strength. Calculating the normalized cross correlation between both transports, a weaker correlation of 0.66 (Y92) suggest that for a year of maximum winter sea ice extent no correlation exists between these passages. However, for a year of minimum winter sea ice extent (Y90) the two transports are strongly correlated (0.97) indicating that water formed on the western continental shelf has less influence on the Philip Passage transport. Thus, Y90 SSR overflow seems to be determined by the WSDW transport within the Weddell Gyre. As the density difference (Y92 minus Y90) in the bottom layer on the western continental shelf off Larsen Ice Shelf (Figure 9) shows, denser water is formed in Y92. Thus, continental shelf water formed in years with minimum winter sea ice extent is indeed less dense contributing less to the Philip Passage transport.
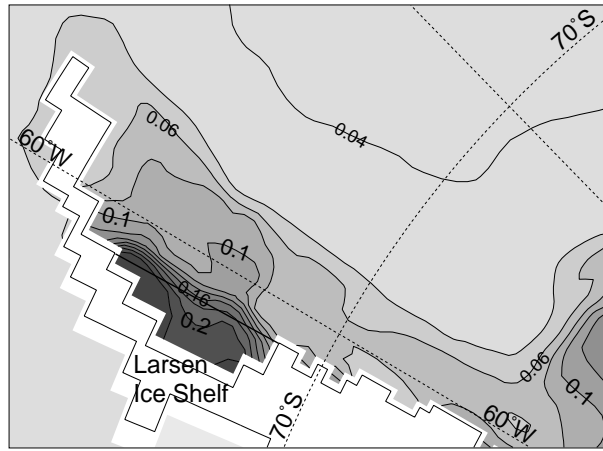
14

Fig. 9. Modelled bottom density differences of the sensitivity runs Y92-Y90 for the western Weddell Sea continental shelf. Positive values indicate higher bottom densities for the year with maximum winter sea ice extent. Contour interval is 0.02 kg m^{-3}.

Various smaller gaps

A series of gaps east of the Orkney Passage (Bruce, Discovery, and Hoyer passages from west to east, see Figure 2) also serve as possible entrances for deep water into the Scotia Sea.

Bruce Passage (BP) being closest to Orkney Passage is deep enough to allow for WSDW throughflow. The model depth of 2800 m is close to the measured depth of 2900 m (Naveira Garabato, pers. comm.). However, a shoaling sea floor to the north of BP prevents the northward advance of WSDW. In contrast to inverse model calculations providing 1.4 Sv $\pm$ 1.2 Sv WSDW export Naveira Garabato et al. (2001b), our model indicates in- and outflow of WSDW of around 0.1 Sv, thus no net northward transport through this gap.

Discovery (DP) and Hoyer passages are not well represented in the model. The interpolation procedure changes the depth and only small amounts of WSDW (several mSv) are exported from the Weddell into Scotia seas at these locations.

Hence, grid spacing for the eastern part of the SSR, although constituting one of the finest grid resolution available to date, still seems to be too large. As mentioned above, the bottom potential temperatures observed in the eastern Scotia Sea suggest that there has to be a flow through narrow gaps east of the Orkney Passage. Therefore, this part of the SSR still conceals an unknown quantity of deep water export to the north.

15

Bransfield Strait

In Bransfield Strait (BS) modelled mean flow shows a westward current for the southern part (Figure 8c). In agreement with the observations, the core transports 2 Sv of cold water von Gyldenfeldt et al. (2001) which derives from the continental shelf east of the Antarctic Peninsula (Gordon et al., 2000). Thus, water recently ventilated off Larsen Ice Shelf prefers a northward spreading route on the continental shelf as shallow boundary current instead of spilling over the continental shelf break. This current ventilates the bottom waters in Bransfield Strait and subsequently the deep southeastern Pacific as the cold water plume extends well into the coastal current found along the continental slope west of the Antarctic Peninsula. The results show a small eastward transport of around 0.1 Sv in the northern part of Bransfield Strait, which is small compared to observations (López et al., 1999; Gordon et al., 2000). The reason for this might be twofold; on the one hand the interpolation procedure for the bottom topography does not maintain the complex bathymetry of Bransfield Strait, i.e., the three deep basin structure. Furthermore, the South Shetland Island complex is far more subtle than achieved by the model allowing water masses to enter Bransfield Strait between, e.g., Smith and Snow Islands from the north (García et al., 1994). On the other hand ECMWF reanalyzed 2-m air temperatures are slightly too high around the tip of the Antarctic Peninsula causing ice free conditions though heavy sea ice was observed (Timmermann et al., 2001). Thus, the role of the Bransfield Strait in replenishing water towards the Weddell Scotia Confluence is underestimated in this model and needs further investigation.

5   Spreading and origin

The intent of this experiment is to determine the origin of water masses crossing the SSR, and to examine the spreading pathways and timescales of water masses from the source regions to the SSR. Two sets of experiments (forward and backward integration mode) were performed using 3-dimensional Lagrangian (numerical) particles. The trajectories of these particles, from here on called floats, are obtained by advecting particles at each time step using the archived 3-day, 3-dimensional velocity fields of the 31st year of integration. Floats were 'released' at the beginning of each month and were advected using a modified fourth-order Runge–Kutta time stepping scheme (Press et al., 1986). The time step is 4 hours, and float locations are recorded every 3 days for the integration period of 5 years. With the backward integration mode we intend to find the source area of water masses flowing through the gaps in the South Scotia Ridge, i.e., areas of convection on the continental shelf. Floats are considered to be in contact with the atmosphere when entering the surface

mixed layer. We required the difference between density at the position of the float and surface density to be ρ_{flt}-$\rho_{surf} \leq 0.01$ kg m^{-3} in order to identify the float position as an area of surface contact.

Pathways from the continental shelf

An ensemble of 18000 floats was released in the bottom layers of the continental slope south of Larsen Ice Shelf (forward mode), since a large number of particles is required to get statistical significant results (Döös, 1995). The floats were released at the beginning of each month over a period of one year, and the trajectories recorded for five years. The release site, located south of the area where Fahrbach et al. (2001) observed a $\sim$ 150 m thick bottom layer with WSBW characteristics, was chosen to simulate the spreading of freshly ventilated water masses into the deep ocean.
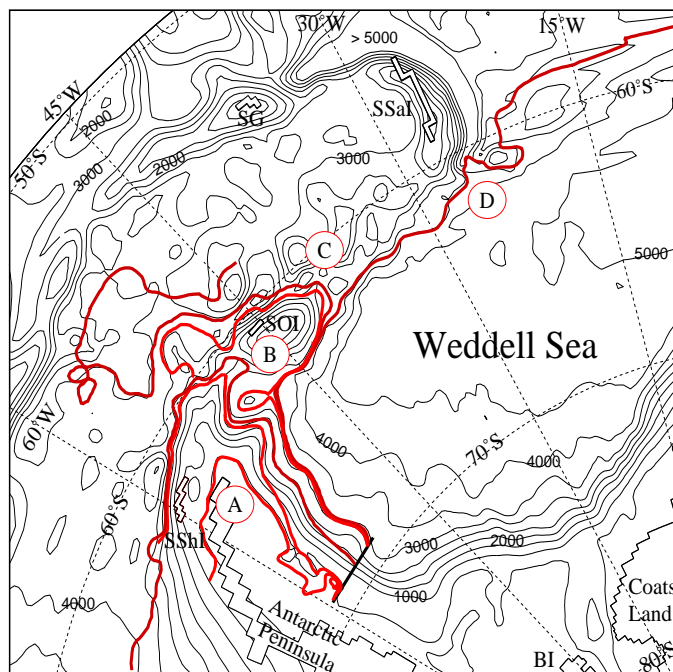

Fig. 10. Mean pathways of particles (N_{total}=216000) released in the bottom boundary layer south of Larsen Ice Shelf. The regions of interest are. **A** – Northwestern Weddell Sea shelf and exit to Bransfield Strait, **B** – Powell Basin and transport across South Scotia Ridge via Philip Passage, **C** – transport across South Scotia Ridge via Orkney Passage, **D** – flow into the deep Weddell abyssal plain. Islands are abbreviated as in Figure 2.

The ensemble mean trajectories show that different spreading routes of WSDW/ WSBW can be distinguished (Figure 10). As known from the flow field, a separation occurs south of Joinville Ridge. One branch descends into the deep ocean while the other remains on the continental shelf. This leaves a zone of

17

low velocities just to the east of the tip of the Antarctic Peninsula von Gylden-feldt et al. (2001), separating the shelf regime from the slope and deep water regimes. The zone does not contain any floats released south of Larsen Ice Shelf. Twelve percent of the floats remain on the continental shelf and subsequently progress west around the tip of the Antarctic Peninsula. While 80 % of these enter Bransfield Strait (BS), the remaining 20 % continue westward north of the SShI. About 210 days after being released floats have travelled to the entrance of BS. A second peak of floats enters BS about 660 days after deployment due to a different continental shelf route with lower velocities away from the shelf break. Floats entering BS are associated with the cold core mentioned in section 4, thus showing the path of water renewing BS deep and bottom waters. Furthermore, water masses rounding the tip of the peninsula propagate further west entering the deep Bellingshausen-Amundsen Sea (adhered to the continental shelf) within the coastal current. Floats entering the Scotia Sea north of SShI move westward before being incorporated and upwelled in the ACC to mid-depth.

The overflow at Philip Passage (B, in Figure 10) reveals two pathways for ventilated waters, the eastern being deeper than the western with a small topographic rise in between these two sub–gaps. Fourty-four percent of the floats released on the continental shelf flow over the SSR through Philip Passage. Since the western part of Philip Passage is closer to the deployment site, it takes 225 days to reach the gap while the travel time to the eastern part, situated closer to the South Orkney Islands, is 350 days. This is documented by the eastern path which almost traverses Powell Basin before being topographically guided north out of the Weddell Sea. Similar to water masses rounding the tip of the Antarctic Peninsula, these floats immediately turn towards Drake Passage. Some of the floats follow the route to the west within the Antarctic coastal current while the remainder upwell and spread with the ACC to the east.

There are two distinct routes from the western Weddell Sea into the Scotia Sea via Orkney Passage (C; 28% of the floats). The shallower route enters the Powell Basin, traverses it and hugs the southern slope of the South Orkney Plateau before leaving the Weddell Sea through Orkney Passage. The deeper route relates to water masses sligthly denser and thus too deep in the water column to cross the sill at the entrance of Powell Basin. However, this water also leaves the Weddell Sea through Orkney Passage. 560 days after the release, the first peak of floats passes through Orkney Passage. 110 days later another peak follows accounting for 80 % of all floats leaving the Weddell Sea through Orkney Passage. The travel-time difference illustrates the different length of the two pathways and emphasizes the importance of the PB sill for the spreading of dense water masses in the northwestern Weddell Sea. Once the water passed through Orkney Passage it turns towards the north/northwest filling the deeper levels of the Scotia Sea. In addition, some flow is directed

towards the southern Drake Passage as observed by *Nowlin and Zenk* [1988] continuing into the South Pacific sector of the Southern Ocean. Subsequently, some of this deep water underrides the ACC. As it upwells, it ventilates the LCDW, i.e., cools and freshens it while returning eastward in the ACC higher in the water column (Locarnini et al., 1993). Additionally, an eastward return flow at the bottom of the Scotia Sea exists, eventually (after more than the 5 years of forward integration) leaving the Scotia Sea through the northwestern part of Georgia Passage (Naveira Garabato et al., 2001a).

The Endurance Ridge, a topographic elevation southeast of the South Orkney Plateau, serves as a dividing site for floats. Part of the floats are topographically guided into Orkney Passage and out of the Weddell Sea while some floats (6 %) remain on a more southerly track towards the deep abyssal plain (D). Dense WSDW and WSBW associated with these floats traversing along the southern slope of the SSR fill the South Sandwich Trench and might be able to enter the Scotia Sea from the northeast.

The remaining 10 % of the floats released south of Larsen Ice Shelf are unaccounted for as they upwell into waters above WSDW and might cross the South Scotia Ridge at higher levels.

Origin of passage waters

Based on the results of the previous section two locations were chosen to the west (Philip Passage) and to the east (Orkney Passage) of South Orkney Islands. Using the archived velocity field in backward mode, we are able to determine the origin of floats released in the dense bottom layer within the passages (Figure 11) as well as the time elapsed since they left the mixed layer. A total of 480000 floats were released (40000 at the beginning of each month). Two major areas of deep convection are identified (Figure 12), the southwestern and southeastern Weddell Sea, the region off the Eastern Weddell Ice Shelves (EWIS, see also Figure 1). However, Figure 12b also indicates that a large portion of WSDW and, thus, of overflow water originates outside the Weddell Sea (Meredith et al., 2000; Schodlok et al., 2001).

Mean travel times as indicated in Figure 12 are based on the first major peak of floats reaching the mixed layer. Depicting the fastest floats they account for roughly 75 % of them. Floats reaching the western sub-gap of Philip Passage have travelled 500 days from the southwestern mixed layer and 755 days from the eastern mixed layer. The time difference of 255 days is caused by the difference in path length. Most of these floats have their origin in winter, the time when the mixed layer is deepest, and in early spring. A similar travel time difference between the southwestern and eastern convection sites of almost
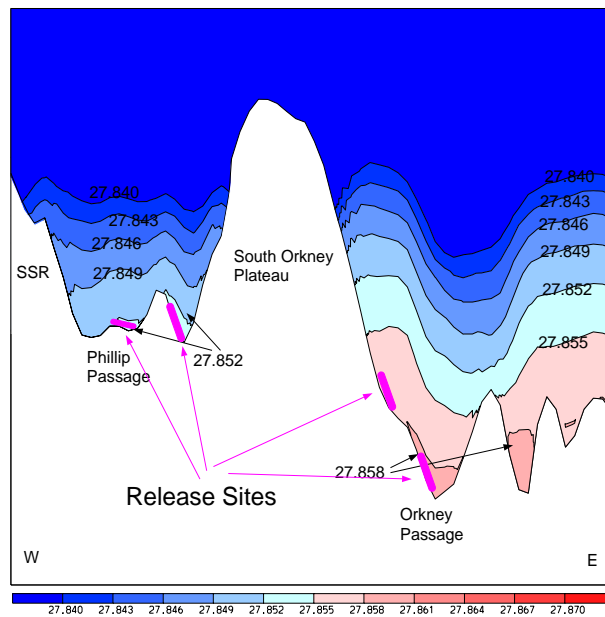
19

Fig. 11. Density section (contour interval $0.003\,\mathrm{kg\,m^{-3}}$) across the sills of the western South Scotia Ridge covering the deepest passages, Philip Passage to the west and the entrance of Orkney Passage to the east of South Orkney Plateau. Marked are the release sites of floats calculated backwards coinciding with the densest waters found in each gap.

9 months exists for those floats released in the eastern sub–gap of Orkney Passage. However, the total travel time for the latter increased by 10 months, corresponding to the time floats need to proceed from Powell Basin to Orkney Passage at mean velocities of $0.03\,\mathrm{m\,s^{-1}}$. Furthermore, Figure 12b shows that Orkney Passage is not ventilated from the southern Weddell Sea continental shelf near Berkner Island, but mainly from shelves further to the east.
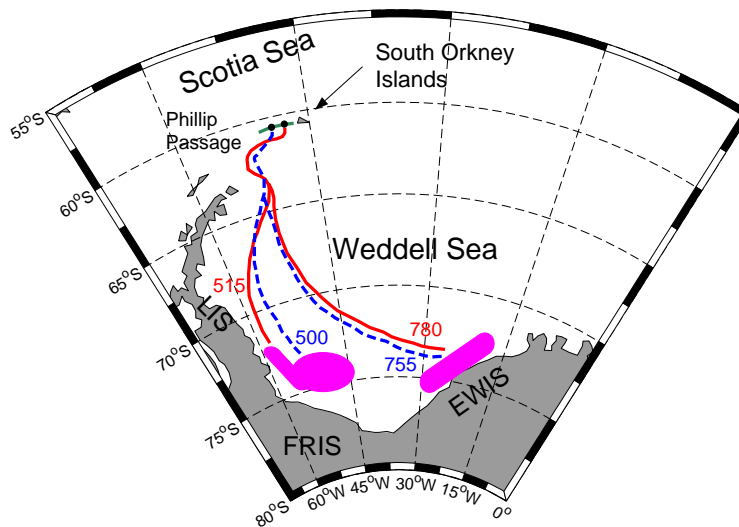

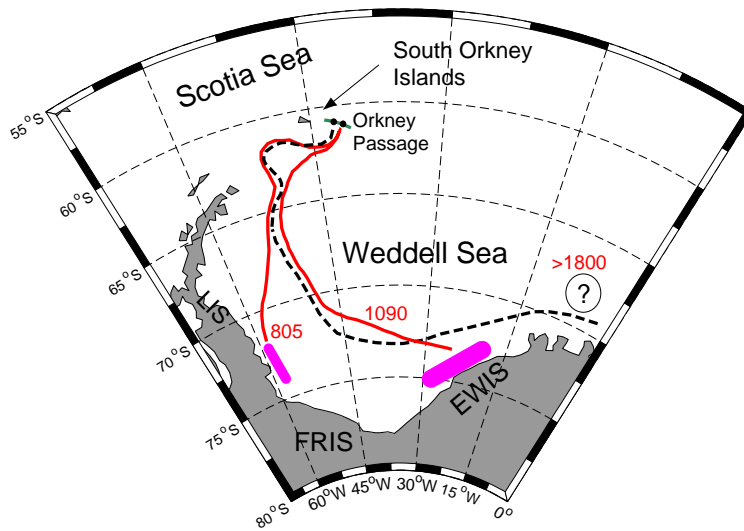Fig. 12. (a) Origin of particles released in Philip Passage, ... continued

Fig. 12. (b) released in Orkney Passage. (a) and (b) resemble mean trajectories of an ensemble of 40000 floats/month. Numbers next to the trajectories represent travel time (in days) from the point of release to the area of deep convection (= near surface contact). LIS: Larsen Ice Shelf; FRIS: Filchner-Ronne Ice Shelf; EWIS: Eastern Weddell Ice Shelves.

6 Discussion and conclusions

Our experiments provide valuable information additional to the observations (e.g., Naveira Garabato et al. (2001b)). They support the hydrographic picture drawn from measurements (e.g., Gordon et al. (2001)) and illustrate for the first time the entire suite of pathways of water masses from the inner Weddell Sea across the South Scotia Ridge into the Scotia Sea.

Weddell Sea Deep Water leaves the Weddell Sea through two major passages. Located to the west of the South Orkney Plateau, Philip Passage (49°W) allows a shallow WSDW component to flow northward at a rate of 2.2 Sv. Deeper and denser outflow into the Scotia Sea occurs via Orkney Passage (40°W) at a rate of 4.2 Sv. In total, 6.4 Sv of WSDW are exported from the Weddell Sea into the Scotia Sea with a mean transport rate of WSDW within the northern limb of the Weddell Gyre of 24 Sv. Smaller passages east of the Orkney Passage do not contribute significantly to the export of WSDW. Among these, Bruce Passage shows a closed circulation suggesting that bottom topography effectively blocks water colder than 0.0°C from flowing north. Since the eastern part of the South Scotia Ridge is not well resolved, as there are sub–grid size clefts, and a flow from the east into the Scotia Sea (Locarnini et al., 1993) exists, this rate of 6.4 Sv can be seen as a lower estimate for the Scotia Sea ventilation.

Orkney and Philip Passage transports exhibit a semi-annual oscillation at a

21

maximum amplitude of $\pm$ 0.4 Sv and $\pm$ 0.2 Sv, respectively. Atmospheric records from Faraday Station (Antarctic Peninsula) show a similar semi–annual oscillation in monthly mean surface pressure indicating maximum cyclonic activity during the equinoctal months (King and Turner, 1997). The transport oscillation in Orkney Passage is more strongly correlated with the WSDW transport in the northern limb of the Weddell Gyre than that in Philip Passage. This suggests that Orkney Passage transports are mainly controlled by Weddell Gyre transports whereas Philip Passage transports are more likely to be influenced by shelf waters entering Powell Basin at Joinville Ridge. However, the model run forced with the 1990 forcing data, the year with minimum winter sea ice extent in the period 1985 to 1993, indicates a good correlation between Orkney Passage and Philip Passage transports. For this year the influence of the shelf regime on the Phillip Passage transport is less pronounced, and the transport is determined by WSDW flow within the Weddell Gyre. This indicates that the influence of the shelf regime depends on the sea ice conditions on the western Weddell Sea continental shelf. Bottom density differences off Larsen Ice Shelf between the two forcing extrema support this notion. In years with maximum winter sea ice extent, denser water masses are formed which descend down the continental slope than in years with minimum winter sea ice extent. Subsequently, these waters enter Powell Basin and are able to leave the Weddell Sea via Philip Passage reducing and obstructing waters entering Powell Basin from the western limb of the Weddell Gyre. The sensitivity studies showed the interannual variability of the WSDW export. Transports increased when the model was forced with 1990 data, i.e., the year of minimum winter sea ice extent (6.9 Sv) while they decreased for 1992 forcing data (6.1 Sv), the year of maximum winter sea ice extent.

A cold core of water progresses from the western Weddell Sea continental shelf into the Bransfield Strait with a rate of 2 Sv. However, only little eastward transport into the Weddell and Scotia seas exist, indicating some limitations of the model.

Forward integrated particle trajectories (n=18000) illustrate the major pathways of water masses formed on the western continental shelf. Seventy-two percent of the floats released in the ventilated bottom layer (Fahrbach et al., 2001) cross the South Scotia Ridge via Phillip Passage (44 %) and Orkney Passage (28 %). The flow on the northwestern continental shelf is divided into a shelf and a deep water regime separated by a zone of low velocities. While the descending floats proceed through Powell Basin into the Scotia Sea and into the deep Weddell Sea, the shelf water exported to Bransfield Strait and southern Drake Passage (12 %) renews Bransfield Strait deep and bottom waters as well as progressing into the deep Amundsen–Bellingshausen Basin. Six percent of the floats are not able to cross the passages in the South Scotia Ridge and advance towards the east into the deep abyssal plains of the Atlantic and Indian oceans. Two topographic features influence the spreading

of bottom waters in the northwestern Weddell Sea; the sill at the gateway to Powell Basin and the Endurance Rige southeast of the South Orkney Plateau. Both are responsible for the divergence of the WSDW flow resulting in different arrival times at the South Scotia Ridge and volumes passing through the gaps. In the Scotia Sea, WSDW is mainly transported with the bottom boundary current along the northern slope of the South Scotia Ridge into the southern Drake Passage and farther west. While underriding the ACC, WSDW upwells and thus ventilates the LCDW, i.e., cools and freshens ACC waters and returns eastward in the ACC higher in the water column. Nevertheless, an eastward return flow also exists at the bottom of the Scotia Sea which might be able to penetrate into Georgia Basin through the northern Georgia Passage.

Lagrangian particle trajectories calculated backwards show that water masses flowing through passages in the South Scotia Ridge mainly originate from the southwestern Weddell Sea continental shelf and from the region off the Eastern Weddell Ice Shelves. Most of the floats leave the source area in winter when the mixed layer is deepest and convection occurs. Weddell Sea Deep Water also seems to derive from the Prydz Bay area, since many floats released in the gaps of the South Scotia Ridge result from ventilation processes outside the Weddell Sea. This agrees well with CFC observations (Meredith et al., 2000; Klatt et al., 2001) and model studies focused on the origin of the deep CFC maximum in the eastern Weddell Sea (Schodlok et al., 2001). However, uncertainties remain about the fate of WSDW entering the inner Weddell Sea within the coastal current. The advective floats suggest that water masses in the depth range of the southern CFC maximum core at Greenwich Meridian circulate through the inner Weddell Sea leaving it through Orkney Passage.

Acknowledgments

References

Beckmann, A., Haidvogel, D. B., 1993. Numerical Simulation of Flow around a Tall Isolated Seamount. Part I: Problem Formulation and Model Accuracy . J. Phys. Oceanogr. **23**, 1736–1753.

Beckmann, A., Hellmer, H. H., Timmermann, R., 1999. A numerical model of the

Weddell Sea: large scale circulation and water mass distribution. J. Geophys. Res. **104**, 23375–23391.

Brennecke, W., 1921. Die ozeanographischen Arbeiten der deutschen antarktischen Expedition 1911–1912. Tech. rep., Arch. Deutsche Seewarte.

Carmack, E. C., 1977. Water characteristics of the Southern Ocean south of the Polar Front. In: A voyage of Discovery. Pergamon, London, pp. 15–41.

Comiso, J. C., Gordon, A. L., 1998. Interannual variability in summer sea ice minimum, coastal polynyas, and bottom water formation in the Weddell Sea. In: M.O. Jeffries (Ed.), Antarctic sea ice: Physical processes, Interactions and Variability. Vol. **74** of Antarc. Res. Ser. AGU, pp. 293–315.

de Zeeuw, P. M., 1990. Matrix–dependent prolongations and restrictions in a black-box multigrid solver. J. Comput. Appl. Math. **33**, 1–27.

Döös, K., 1995. Interocean exchange of water masses. J. Geophys. Res. **100**, 13499–13514.

Fahrbach, E., Harms, S., Rohardt, G., Schröder, M., Woodgate, R., 2001. Flow of bottom water in the northwestern Weddell Sea. J. Geophys. Res. **106**, 2342–2365.

Fahrbach, E., Rohardt, G., Krause, G., 1992. The Antarctic Coastal Current in the southeastern Weddell Sea. Polar Biol. **12**, 171–182.

García, M. A., López, O., Sospedra, J., Espino, M., Gràcia, V., Morrison, G., Rojas, P., Figa, J., Puigdefàbregas, J., S.-Arcilla, A., 1994. Mesoscale variability in the Bransfield Strait region (Antarctica) during Austral summer. Annales Geophys. **12**, 856–867.

Georgi, D. T., 1981. Circulation of bottom waters in the southwestern South Atlantic. Deep-Sea Res. **28A** (9), 959–979.

Gill, A. E., 1973. Circulation and bottom water production in the Weddell Sea. Deep-Sea Res. **20**, 111–140.

Gordon, A. L., 1966. Potential Temperature, Oxygen and Circulation of Bottom Water in the Southern Ocean. Deep-Sea Res. **13**, 1125–1138.

Gordon, A. L., Mensch, M., Dong, Z., W. M. Smethie, J., de Bettencourt, J., 2000. Deep and bottom water of the Bransfield Strait eastern and central basins. J. Geophys. Res. **105**, 11337–11346.

Gordon, A. L., Visbeck, M., Huber, B., 2001. Export of Weddell Sea Deep and Bottom Water. J. Geophys. Res. **106**, 9005–9017.

Haidvogel, D. B., Wilkin, J. L., Young, R. E., 1991. A semi-spectral primitive equation ocean circulation model using vertical sigma and orthogonal curcilinear horizontal coordinates . J. Comput. Phys. **94**, 151–185.

Hellmer, H. H., Jacobs, S. S., Jenkins, A., 1998. Oceanic Erosin of a floating Antarctic glacier in the Amundsen Sea . In: S.S. Jacobs (Ed.), Ocean, Ice, and Atmosphere: Interactions at the Antarctic Continental Margin. Vol. **75** of Antarc. Res. Ser. AGU, pp. 83–99.

Hibler, III, W. D., 1979. A dynamic-thermodynamic sea ice model. J. Phys. Oceanogr. **9**, 815–846.

Jackett, D. R., McDougall, T. J., 1995. Stabilization of hydrographic data. J. Atmos. Oceanic Technol. **12**, 381–389.

Johnson, M. R., Smith, A. M., 1997. Seabed topography under the southern and western Ronne Ice Shelf, derived from seismic surveys. Antarctic Science **9**, 201–208.

King, J. C., Turner, J., 1997. Antarctic meteorology and climatology. Cambridge University Press.

Klatt, O., Roether, W., Hoppema, M., Bulsiewicz, K., Fleischmann, U., Rodehacke, C., Fahrbach, E., Weiss, R. F., Bullister, J., 2001. Repeated CFC sections at the Greenwich Meridian in the Weddell Sea. J. Geophys. Res. Submitted.

Lemke, P., Owens, W. B., W. D. Hibler, I., 1990. A coupled sea-ice mixed layer-pycnocline model for the Weddell Sea. J. Geophys. Res. **95**, 9512–9525.

Locarnini, R. A., T. Whitworth, I., W. D. Nowlin, J., 1993. The importance of the Scotia Sea on the outflow of Weddell Sea Deep Water. J. Mar. Syst. **51**, 135–153.

López, O., García, M. A., Gomis, D., Rojas, P., Sospedra, J., Sánchez-Arcilla, A., 1999. Hydrographic and hydrodynamic characteristics of the eastern basin of the Bransfield Strait (Antarctica). Deep-Sea Res. **46**, 1755–1778.

Meredith, M. P., Locarnin, R. A., Scoy, K. A. V., Watson, A. J., Heywood, K. J., King, B. A., 2000. On the sources of Weddell Gyre Antarctic Bottom Water. J. Geophys. Res. **105**, 1093–1104.

Muench, R. D., Hellmer, H. H., 2001. The DOVETAIL program: introduction to the special collection. Deep-Sea Res. this issue.

Naveira Garabato, A. C., Heywood, K. J., Stevens, D. P., 2001a. Modification and pathways of the deep waters of the Antarctic Circumpolar Current in the Scotia Sea. Deep-Sea Res. , submitted.

Naveira Garabato, A. C., McDonagh, E. L., Stevens., D. P., Heywood, K., Sanders, R., 2001b. On the export of Antarctic Bottom Water from the Weddell Sea. Deep-Sea Res. this issue.

Olbers, D. J., Gouretski, V., Seiß, G., Schröter, J., 1992. Hydrographic Atlas of the Southern Ocean. Alfred-Wegener-Institut, Bremerhaven, 82 pp.

Orsi, A. H., T. Whitworth, I., W. D. Nowlin, J., 1995. On the meridional extent and fronts of the Antarctic Circumpolar Current. Deep-Sea Res. **42**, 641–673.

Orsi, A. H., W. D. Nowlin, J., T. Whitworth, I., 1993. On the circulation and stratification of the Weddell Gyre. Deep-Sea Res. **45**, 269–301.

Pacanowski, R. C., Philander, S. G. H., 1986. A model of the seasonal cycle in the tropical Atlantic Ocean. J. Geophys. Res. **91**, 14192–14206.

Press, W. H., Flannery, B. P., Teukolsky, S. A., Vetterling, W. T., 1986. Numerical recipes, the art of scientific computing. Cambridge University Press.

Rakowsky, N., 1999. Efficient parallel solvers for elliptic partial differential equations arising in numerical ocean modelling. Reports on polar research, 318, AWI, Bremerhaven, 154 pp.

Schodlok, M. P., Rodehacke, C. B., Hellmer, H. H., Beckmann, A., 2001. On the origin of the deep CFC maximum in the eastern Weddell Sea – numerical model results. Geophys. Res. Let. **28**, 2859–2862.

Schröder, M., Fahrbach, E., 1999. On the structure and transport of the eastern Weddell Gyre. Deep-Sea Res. **46**, 501–527.

Schröder, M., Hellmer, H. H., Absy, J. M., 2001. Near-bottom variability in the northwestern Weddell Sea. Deep-Sea Res. this issue.

Smith, W. H. F., Sandwell, D. T., 1997. Global Sea Floor Topography from Satellite Altimetry and Ship Depth Soundings. Science **277**, 1956–1962.

Smythe-Wright, D., Boswell, S., 1998. Abyssal circulation in the Argentine Basin. J. Geophys. Res. **103**, 15845–15851.

Timmermann, R., Hellmer, H. H., Beckmann, A., 2001. Simulations of ice-ocean dynamics in the Weddell Sea. Part II: Interannual variability 1985 – 1993. J. Geophys. Res. In press.

von Gyldenfeldt, A.-B., Fahrbach, E., García, M., Schröder, M., 2001. Flow variability at the tip of the Antarctic Peninsula. Deep-Sea Res. this issue.

White, W. B., Peterson, R. G., 1996. An Antarctic circumpolar wave in surface pressure, wind, temperature and sea–ice extent . Nature **380**, 699–702.

Whitworth, III, T., Orsi, A. H., Kim, S. J., Nowlin, Jr., W. D., Locarnini, R. A., 1998. Water masses and mixing near the Antarctic Slope Front. In: S.S. Jacobs and R.F. Weiss (Ed.), Ocean, Ice and Atmosphere: Interactions at the Antarctic Continental Margin. Vol. **75** of Antarc. Res. Ser. AGU, pp. 1–27.

Whitworth, III, T., Peterson, R. G., 1985. The volume transport of the Antarctic Circumpolar Current from three-year bottom pressure measurements. J. Phys. Oceanogr. **15**, 810–816.